On the Mechanical Properties of Chiral Carbon Nanotubes

M. Zakeri[1], M. Shayanmehr[1]

Abstract

Carbon nanotubes (CNTs) are specific structures with valuable characteristics. In general, the structure of each nanotube is defined by a unique chiral vector. In this paper, different structures of short single-walled CNTs are simulated and their mechanical properties are determined using finite element method. For this aim, a simple algorithm is presented which is able to model the geometry of single-walled CNTs with any desired structure based on nano-scale continuum mechanics approach. By changing the chiral angle from 0 to 30 degree for constant length to radius ratio, the effect of nanotube chirality on its mechanical properties is evaluated. It is observed that the tensile modulus of CNTs changes between 0.93-1.02 TPa for different structures, and it can be higher for chiral structures than zigzag and armchair ones. Also, for different chiral angles, the bending modulus changes between 0.76-0.82 TPa, while the torsional modulus varies in the range of 0.283-0.301TPa.

Keywords: Carbon Nanotube; Chirality; Tensile Rigidity; Bending Rigidity; Torsional Rigidity

1. Introduction

Many researchers employed numerical approaches including molecular dynamics (MD) and continuum mechanics to simulate CNTs structures. In recent decades, continuum mechanics approaches based on finite element method (FEM) have been widely used to evaluate the elastic properties of CNTs via micromechanical methods. Different types of finite elements, including rods, trusses, springs, and beams using linear and nonlinear interatomic potentials have been utilized to model the carbon–carbon (C–C) bond in CNTs [e.g. 3-6]. For example, Meo and Rossi [3] simulated CNT using non-linear spring for modeling the bond stretch, and linear torsional spring for modeling the bond angle variation. In this model, bending of a bond is surrounded using additional elements as diameters of the hexagon.

Li and Chou [7] stated that a CNT is a geometrical frame-like structure and the primary covalent bonds between two nearest-neighboring atoms act like load-bearing beam elements, whereas the atoms act as the joints of the related beam members. By establishing a linkage between structural mechanics and molecular mechanics, they determined the sectional properties of these beam members. Tserpes et al. [8, 9] used beam elements based on linear and nonlinear interatomic potentials. They concluded that Young's modulus of chiral CNTs is larger than zigzag and armchair structures. Giannopoulos et al. [10] explored the mechanical properties of CNTs by using spring elements. They used atomistic microstructure of CNTs and found that armchair nanotubes provide slightly higher values of Young's modulus and lower values of shear modulus than zigzag ones for small values of radius, and the results tented to converge for higher values of radius. However, Ávila and Lacerda [11] reported that Young's modulus of zigzag is larger than armchair and chiral structures.

In 2012, Rafiee and Heidarhaei [12] studied the effect of structure type (only armchair and zigzag) on Young's modulus (E) of CNTs. They presented a brief summary of some previously published values for E obtained from different approaches of MD and FEM, and claimed that the Young's modulus of CNTs is independent of their structure. In another research, Lu and Hu [13] investigated the mechanical properties of three structures of armchair, zigzag and chiral with angle of 19.1

1- Aerospace Engineering Department, K. N. Toosi University of Technology, Tehran, 16569-83911, Iran. Tel.: +98-21-73064217; fax: +98-21-77791045.

Corresponding author:
M. Zakeri, Aerospace Engineering Department, K. N. Toosi University of Technology, Tehran, 16569-83911, Iran. Tel.: +98-21-73064217; fax: +98-21-77791045.
Email: m.zakeri@kntu.ac.ir

degree, and reported that the largest Young's modulus is calculated for zigzag CNT. Also, they reported that the shear modulus increases as the chiral angel increases.

Although extensive studies have been done to explore the mechanical properties of carbon nanotubes; most of these studies have been restricted only to symmetric structures of CNTs including zigzag and armchair ones. In this paper, short CNTs with any desired structure are modeled using a new developed simple algorithm based on nanoscale continuum mechanics. Then, these models are analyzed using finite element method to examine the mechanical behavior of CNTs under different loading conditions including tension, bending, and torsion in order to determine the effect of chiral angle on the mechanical properties. In the following section, details of the CNTs modeling technique are described.

2. Modeling of Carbon Nanotubes

2.1. Carbon Nanotube Geometry

A single-walled carbon nanotube (SWCNT) can be considered as a rolled up rectangular plane of graphene layer in shape of a hollow cylindrical tube (Fig. 1). Graphene sheets are flat thin plates consisted of carbon atom bonds in a lattice of regular hexagons. In this structure, each carbon atom has a covalent C–C bond with three other atoms. A roll-up vector is defined in the graphene sheet using two points of the lattice (Fig. 2). The roll-up vector ($\boldsymbol{C_h}$), commonly called chiral vector, determines the direction along which the graphene sheet is rolled to form a tubular CNT structure. This vector can be expressed as:

$$\boldsymbol{C_h} = n\,\boldsymbol{a_1} + m\,\boldsymbol{a_2} \qquad (1)$$

where the indices (n,m) are integer values called the chiral index of nanotube, and $\boldsymbol{a_1}$, $\boldsymbol{a_2}$ are unit vectors of the lattice. A pair of integers (n,m) describes a single-walled nanotube uniquely, and other geometrical parameters of CNT such as its diameter (D) and chiral angle (θ) can be calculated using m and n according to [14]:

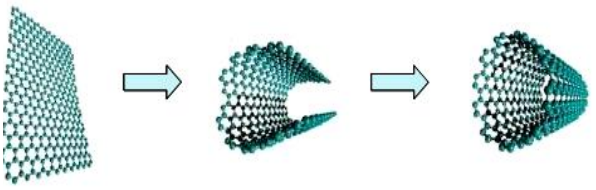

Fig. 1. Rolling up a graphene sheet to form a carbon nanotube

$$D = \left(\frac{\sqrt{3}\,a}{\pi}\right)\left(m^2 + mn + n^2\right)^{1/2} \qquad (2)$$

$$\theta = \tan^{-1}\left[\left(\sqrt{3}\,m\right)\Big/\left(m + 2n\right)\right] \qquad (3)$$

where a is lattice parameter that is the nearest neighbor carbon atom distance, taken as 1.42 angstrom.

Because of hexagonal symmetry of the honeycomb lattice and the chiral symmetry of (n,m) and (m,n) tubes, chiral angles to describe all CNTs are limited to the range of $0 \le \theta \le 30$. Regarding to the size of chiral angle, two particular types of nanotube configurations are created which are symmetric with respect to the tube axis: zigzag nanotube with m = 0 (0-degree structure); and armchair nanotube with $n = m$ (30-degree structure). All the remaining asymmetric structures with arbitrary values of $0 < \theta < 30$ are known as chiral nanotubes [15].

For modeling a carbon nanotube with different structures of zigzag, armchair and desired chiral angle, a precise algorithm for programming is needed. In the currently developed algorithm, first, the chiral angle and other required parameters for creating the geometric model are calculated by receiving three input data of n, m and L (nanotube length). Then, a formula is derived and used for determining the coordinates of graphene sheet points which specifies the situation of each carbon atom. For this purpose, the coordinates of initial reference atom are considered as the starting point and the coordinates of its three neighbor points are calculated. Then, each determined neighbor atom is considered as a new reference point and the calculations are repeated for determining the coordinates of other atoms.

For these calculations, two main groups of Type-1 and Type-2 points are defined regarding to their situation. Fig. 2 shows the way of selecting Type-1 and Type-2 points in

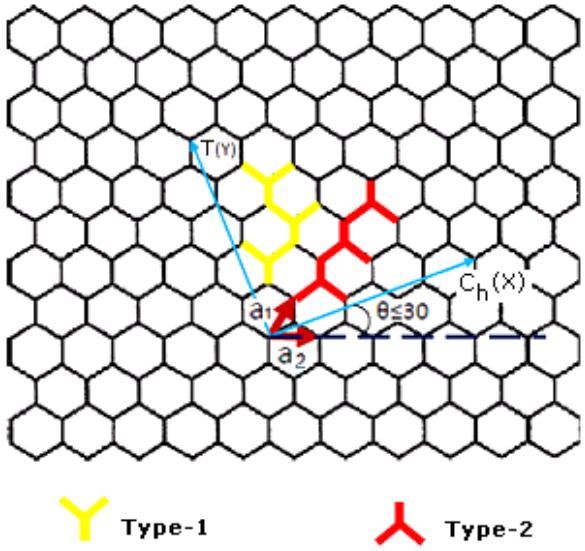

Fig. 2. Type-1 and Type-2 points in the graphene sheet to determine the neighbor atoms position

the graphene sheet. The relations between the coordinates of reference points and new points are derived according to equations 4 to 7. Expressions 4 and 5 are used for Type-1 points and expressions 6 and 7 are used for Type-2 points:

$$X_n = X_0 + a \times \cos\left[-90 + 120\,(i-1) - \theta\right]; \quad i = 1,2,3 \tag{4}$$

$$Y_n = Y_0 + a \times \sin\left[-90 + 120\,(i-1) - \theta\right]; \quad i = 1,2,3 \tag{5}$$

$$X_n = X_0 + a \times \sin\left[-30 + 120\,(i-1) - \theta\right]; \quad i = 1,2,3 \tag{6}$$

$$Y_n = Y_0 + a \times \sin\left[-30 + 120\,(i-1) - \theta\right]; \quad i = 1,2,3 \tag{7}$$

where X_n and Y_n are coordinates of the neighbor point while X_0 and Y_0 are coordinates of the reference atom in Cartesian coordinate system. After determining the coordinates of all points and generating the bonds between them, the prepared model is transferred to three-dimensional cylindrical coordinate system to obtain the final structural model of carbon nanotube.

In this research, all of the above described steps to determine the location of carbon atoms and create the nanotube geometric model have been prepared as a computer code. Fig. 3 shows a flowchart of this code which simulates SWCNTs with any desired dimension and structure. Finally, this model is exported to commercial finite element software ANSYS12 to analyze the nanotube static behavior and examine its mechanical properties.

2.2. Finite Element Modeling of CNTs

Based on the structural mechanics approach developed by Li and Chou [7] the existing covalent force between two carbon atoms of CNT can be simulated by using a beam element which bears all three types of tensile, bending and torsion deformations.

At the molecular level, the interaction between atoms is described based on molecular potential energies. Although nanotubes are structures with nonlinear behavior, chemical calculations have shown that for studying molecular networks under small deformations, bonding potential energy can be well approximated by simple harmonic functions [16]. Inter-molecular potential energy of covalent bonds (E_{total}) can be calculated by using harmonic functions according to relation (8):

$$E_{total} = \frac{1}{2}k_r(\Delta r)^2 + \frac{1}{2}k_\theta(\Delta\theta)^2 + \frac{1}{2}k_\phi(\Delta\phi)^2 \tag{8}$$

where k_r, k_θ, and k_ϕ are bond stretching, bond angle bending and torsional resistance force constants, and Δr, $\Delta\theta$ and $\Delta\phi$ represent the variations of bond lengths, bending angle and twisting angle, respectively.

On the other hand, according to the physical similarity between the molecular energy and structure strain energy, the constants k_r, k_θ and k_ϕ are obtained as:

$$k_r = \frac{E_{el}A_{el}}{a} \quad , \quad k_\theta = \frac{E_{el}I_{el}}{a} \quad , \quad k_\phi = \frac{G_{el}J_{el}}{a} \tag{9}$$

Equations 9 create the basis for replacement of C–C bonds in the graphene sheet and carbon nanotube with a continuous frame-like

structure. The bond equivalent beam characteristic parameters such as its length (a), cross sectional area (A_{el}), moments of inertia (I_{el}, J_{el}), Young's modulus (E_{el}), and torsional modulus (G_{el}) are derived based on the force constants of molecular mechanics field. k_r, k_θ and k_ϕ are equal to 6.52×10^{-7} N/nm, 8.76 $\times10^{-10}$ N.nm/ rad^2, and 2.78×10^{-10} N.nm/rad^2, respectively [8].

In this research, the covalent bonds between carbon atoms of CNT are modeled with linear beam elements including shear effects using ANSYS software.

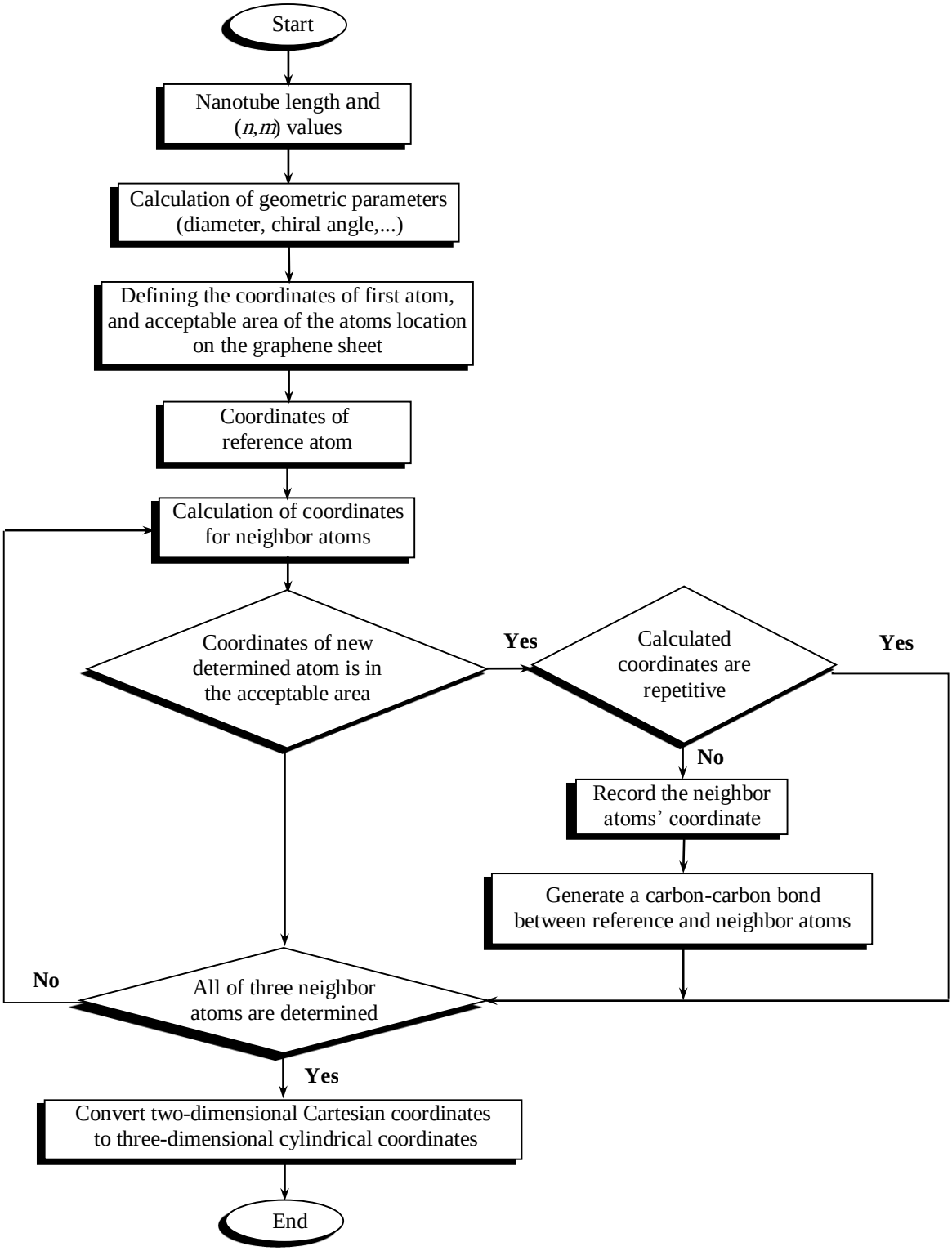

Fig. 3. Flowchart of the algorithm used for CNT geometric modeling.

Table 1. Geometrical and mechanical properties of beam element used to simulate the bond between carbon atoms in finite element model

Element Parameters	Formulation [8]	Quantity
Element/bond length (a)	--------	1.42 (A)
Element diameter (d)	$d = 4\sqrt{k_\theta / k_r}$	1.46 (A)
Elasticity modulus (E_{el})	$E_{el} = \frac{k_r^2 a}{4\pi k_\theta}$	5.48 (TPa)
Torsional modulus (G_{el})	$G_{el} = \frac{k_r^2 k_\phi a}{8\pi k_\theta^2}$	0.87 (TPa)

The geometrical and mechanical properties of the element are selected as Table 1. By assuming a solid circular cross section, cross sectional area (A_{el}) and moments of inertia (I_{el}, J_{el}) could be calculated as $A_{el} = \pi d^2/4$, $I_{el} = \pi d^4/64$ and $J_{el} = \pi d^4/32$. Fig. 4 shows three samples of simulated nanotubes with different structures of zigzag, chiral, and armchair. After generating FE models of CNTs, they are subjected to three different load cases of tension, bending, and torsion.

Table 2. Characteristics of the simulated CNTs.

Structural Group	Chiral Index (n,m)	Chirality (Θ^o)	Radius (A)	Length (A)
(12,m)	(12,0)	0	4.69	25.64
	(12,1)	3.96	4.90	27.63
	(12,3)	10.89	5.38	29.81
	(12,6)	19.10	6.21	33.94
	(12,9)	25.28	7.14	40.38
	(12,12)	30	8.13	46.77
(15,m)	(15,0)	0	5.87	32.
	(15,2)	6.18	6.30	34.8
	(15,5)	13.90	7.06	39.5
	(15,6)	16.10	7.33	42.64
	(15,8)	20.03	7.92	44.86
	(15,12)	26.32	9.17	52.07
	(15,15)	30	10.17	58.96
(18,m)	(18,0)	0	7.04	38.39
	(18,3)	7.59	7.70	43.52
	(18,6)	13.90	8.47	48.44
	(18,9)	19.10	9.32	53.25
	(18,12)	23.41	10.23	59.12
	(18,15)	27	11.20	64.56
	(18,18)	30	12.20	70.09

3. Result and Discussion

3.1. Results for Different Chiral Angles

In this study, all CNT structures with the same value of n and different chiral angles are considered as a structural group, for briefness. For example, (12,0) ,(12,3), (12,6), (12,9), and (12,12) CNTs are referred as structural group of (12,m), and their chiral angle varies from 0 to 30 degree by increasing the value of m. Three structural groups of (12,m), (15,m), and (18,m) CNTs are simulated and analyzed using FEM. All of the modeled CNTs have approximately the same length to radius ratio. Table 2 shows the characteristics of the modeled CNTs.

3.1.1. Tensile Behavior

Tensile behavior of each nanotube is investigated by applying a small tensile axial displacement at one of its ends, while the other end is restricted to move (Fig. 4). Then, the

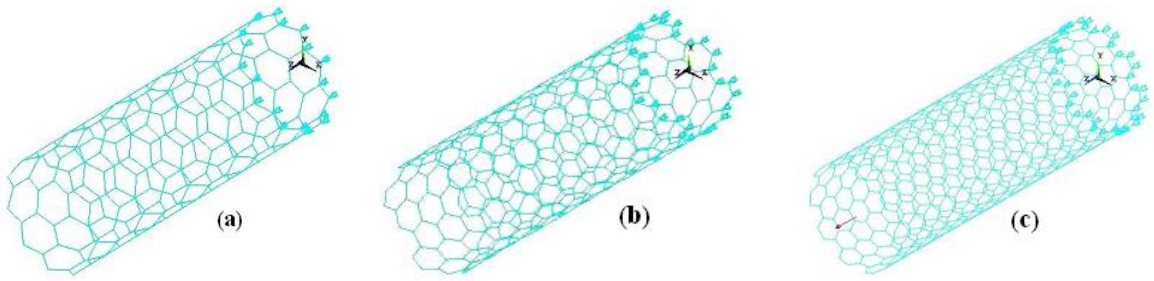

Fig. 4. Samples of FEM models of CNTs with different structures: a) zigzag, b) chiral, c) armchair.

maximum axial force amount at the fixed end of nanotube is calculated using FEM method. Consequently, tensile Young's modulus in the longitudinal direction (E_T) can be calculated using equation 10 based on the linear relationship between stress and strain:

$$E_T = \frac{FL}{\Delta L.A} \qquad (10)$$

where L, ΔL, A and F are nanotube length, changes in nanotube length, cross sectional area, and axial force, respectively. For a CNT with radius of R and wall thickness of t=0.34 nm, cross sectional area is calculated as:

$$A = \pi\left(R_{out}^2 - R_{in}^2\right) \qquad (11)$$

in which $R_{out} = R + t/2$ and $R_{in} = R - t/2$.

Figs. 5-7 present the variation of longitudinal elasticity modulus for different structures of CNTs. Also, applying the cross sectional area, tensile rigidity ($E_T A$) for three structural groups of CNTs is obtained according to Fig. 8. It is observed that the nanotube's tensile rigidity increases rapidly by increasing the chiral angle in a structural group, and in general, its amount for armchair structure has been about 80 percent higher than that of zigzag one. Moreover, according to Fig. 8, increasing the number of atomic networks in the structures causes increasing of tensile rigidity. By considering the impact of both factors, tensile stiffness of studied nanotubes is variable in the range of 4100 AN to 11000 AN.

3.1.2. Bending Behavior

To simulate the bending condition, the free end of CNT is subjected to a small transverse displacement (δ). After applying the bending movement, amount of the maximum force perpendicular to cross section at the fixed support nodes of nanotube is reported by ANSYS software. Then, the bending elasticity modulus (E_B) can be calculated from:

$$E_B = \frac{FL^3}{3I.\delta} \qquad (12)$$

where F, L, δ and I are bending force, CNT length, deflection amount of free end, and the second moment of inertia, respectively. The changes in bending elasticity modulus for

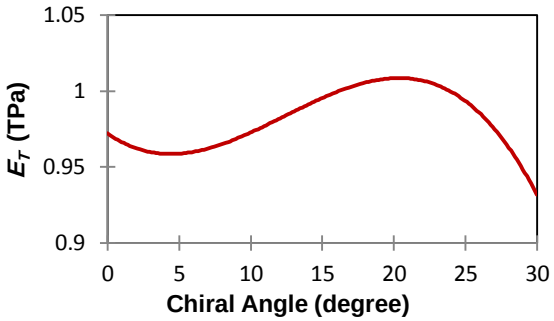

Fig. 5. Variation of longitudinal Young's modulus vs. chiral angle for (12,*m*) CNTs.

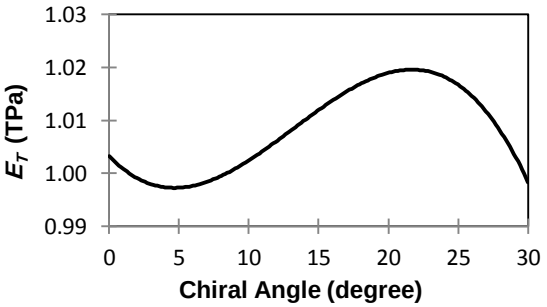

Fig. 6. Variation of longitudinal Young's modulus vs. chiral angle for (15,*m*) CNTs.

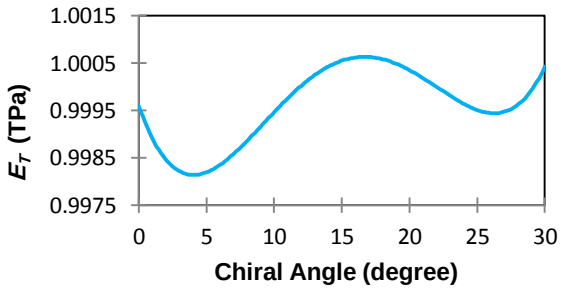

Fig. 7. Variation of longitudinal Young's modulus vs. chiral angle for (18,*m*) CNTs.

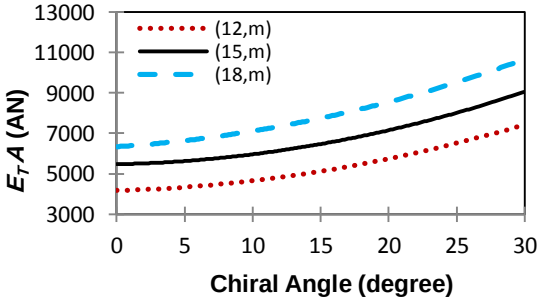

Fig. 8. Variation of CNT tensile rigidity vs. chiral angle.

different structures of nanotubes are illustrated in Fig. 9 for three structural groups.

After computing elasticity modulus in bending state, the amount of bending rigidity ($E_B\ I$) is calculated, and the accomplished results are presented in Fig. 10. It is observed that $E_B\ I$ is variable between 0.39 $\times 10^6$ AN.A m^2 to 6.38 $\times 10^6$ AN.Am^2 based on the CNT structure. By increasing the chiral angle for a particular structural group, the bending rigidity is increased intensively. For example, in the (18, *m*) group, its amount for armchair structure is 6.38 $\times 10^6$ AN.Am^2 that is five times more than 1.25 $\times 10^6$ AN.Am^2 obtained for zigzag structure. Also, comparing different structural groups in Fig. 10 indicates that increasing the number of atomic networks of structures leads to increase in bending rigidity.

3.1.3. Torsional Behavior

For applying torsional condition on nanotubes, Cartesian coordinates are changed to cylindrical coordinates. Then, a small twist angle is applied to the free end of CNT while the other end is fixed. After applying the torsion, the amount of created torsional torque at the constrained end of CNT is determined and torsional modulus *G* is calculated from:

$$G = \frac{TL}{J\varphi} \qquad (13)$$

where *T*, *L*, *J* and φ are torsional moment, nanotube length, polar moment of inertia and twist angle, respectively. Fig. 11 shows the variations of *G* for different structures of CNTs for three structural groups. Also, the amount of torsional rigidity (*GJ*) is calculated according to Fig. 12. It is observed that by increasing chiral angle, torsional rigidity is increased intensively. For (12,*m*) group, its amount for armchair structure is 1.42×10^6 AN.Am^2 which is over five times larger than 0.27×10^6 AN.Am^2 for zigzag structure. Comparing different structural groups indicates that the torsional rigidity is increased by increasing the number of atomic networks of structures.

3.2. Discussions

Based on the results of this research, the structure type has not a significant effect on the amount of the tensile Young's modulus of short CNTs. E_T for different structures of

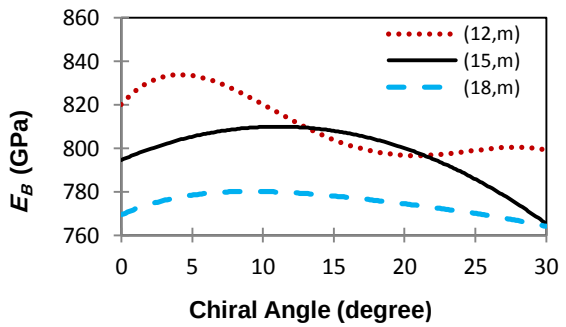

Fig. 9. Variation of bending elasticity modulus vs. chiral angle for three groups of CNTs.

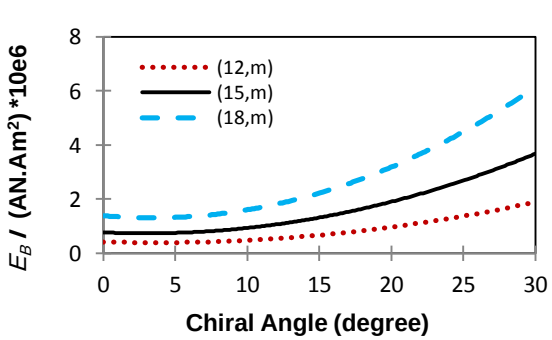

Fig. 10. Variation of CNT bending rigidity vs. chiral angle.

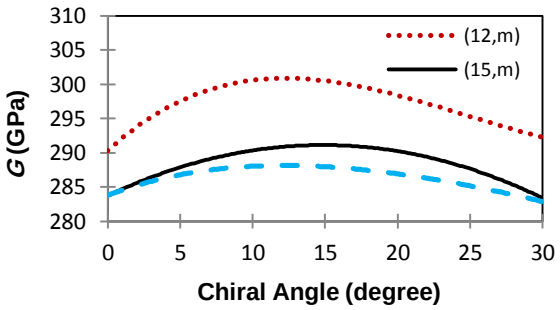

Fig. 11. Variation of torsional modulus vs. chiral angle for three groups of CNTs.

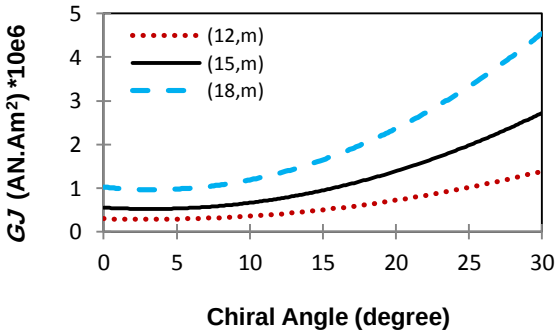

Fig. 12. Variation of CNT torsional rigidity vs. chiral angle

studied CNTs changes from 0.93TPa to 1.02 TPa by changing their structure, and it is generally around 1 TPa. Figs. 5-7 indicates that for (12, *m*) and (15, *m*) nanotubes, zigzag structure is a slighty stiffer than armchair one. In contrast, for (18, *m*) nanotubes, armchair structure has a Young's modulus larger than zigzag one. In this group, armchair CNT is the stiffest structure.

The bending modulus of the studied nanotubes has always been lower than their tensile modulus. According to Fig. 9, bending modulus of nanotubes varies between 0.76TPa to 0.82TPa; and it has a higher value for zigzag structure in comparison with armchair one in a particular structural group. For example, its amount for armchair structure in the (15, *m*) group is 0.764TPa that is a bit less than 0.794TPa obtained for zigzag structure. Also, comparing different structural groups in Fig. 6 indicates that increasing the number of atomic network of structures, generally leads to decrease in bending modulus.

Based on the results presented in Fig. 11, although shear modulus (*G*) of chiral nanotubes is a little more than symmetric ones, it does not change significantly by changing nanotubes structure and increasing the chiral angle. Also, its value for zigzag CNT is very near to armchair structure. In general, torsional modulus is variable from minimum value of 282.86MPa for (18, 18) nanotube to maximum of 300.82MPa for (12, 3) structure, and average torsional modulus for different nanotubes is about 0.29TPa. As another result, comparing different structural groups indicates that by increasing the number of atomic networks of structures the torsional modulus is decreased.

Table 3 shows a summary of the results of this research, in comparison with available reported values for tensile, bending, and torsional moduli of CNTs from literature. It is observed that the overall trend of the present results agrees well with the results reported previously.

4. Conclusions

In this paper, three groups of short carbon nanotubes with different structures were simulated using a simple algorithm. These models were analyzed using finite element method in order to evaluate their mechanical properties including tensile, bending, and torsional modulus and rigidity. By changing chiral angle from $\theta = 0°$ (zigzag) to $\theta = 30°$ (armchair) the effect of CNT structure on its mechanical properties was investigated. The obtained results can be concluded as:

1- The tensile modulus of studied nanotubes changes between 0.93TPa and 1.02TPa for different structures, and it can be higher for chiral CNTs than zigzag and armchair ones.

2- The bending modulus of CNTs changes between 0.76TPa to 0.82TPa. In general, the bending modulus decreases by increasing the number of atomic networks of structures.

3- The torsional modulus of CNTs varies in the range of 0.283TPa to 0.301TPa. Also, similar to bending modulus, the torsional modulus decreases by increasing the number of atomic networks (*n*).

4- Tensile rigidity ($E_T A$), bending rigidity ($E_B I$), and torsional rigidity (GJ) of CNTs were calculated. It is observed that all of these parameters increase intensively by increasing the chiral angle from 0 to 30 degree.

Table 3. The obtained results in comparison with previous results available in the literature.

Tensile Modulus (TPa)	Wernik et al [17]	Shokrieh et al.[18]	Lu et al. [13]	Present Work
	Zigzag: 0.9202 Armchair: 0.9448	1.033-1.042	1.067-1.197	0.93-1.02
Bending Modulus (TPa)	Ayatollahi et al. [19]	Poncharal et al. [20]	Wong et al. [21]	Present Work
	Zigzag: 0.83 Armchair: 0.74-1.3	0.1-1	0.78- 1.78	0.76-0.82
Torsional Modulus (TPa)	Wernik et al [17]	Wu et al [22]	Lu et al. [13]	Present Work
	Zigzag: 0.3442 Armchair: 0.3434	0.418	0.237-0.469	0.283-0.301

References

1. Iijima, S., *Nature*, Vol. 354 (1991) pp. 56-58.
2. Ruoff, R.S., Qian, D., Liu, W.K., *CR Physique*, Vol. 4 (2003) pp. 993–1008.
3. Meo, M., Rossi, M., *Composites Science and Technology*, Vol. 66 (2006) pp.1597–1605.
4. Nahas, M.N., Abd-Rabou, M., *Int. Journal of Mechanical & Mechatronics IJMME-IJENS*, Vol. 10, No. 3 (2010) pp.19-24.
5. Wan, H., Delale, F., *Meccanica*, Vol. 45 (2010) pp. 43–51.
6. Joshi, U.A., Sharma, Satish C., Harsha, S.P., *Physica E*, 45 (2012) pp. 28–35.
7. Li, C., Chou, T.W., *Int J Solids and Structures*, Vol. 40 No. 10 (2003) pp.2487–99.
8. Tserpes, K.I., Papanikos, P., *Composites: Part B*, Vol. 36 (2005) pp.468–77.
9. Tserpes, K.I., Papanikos, P., Tsirkas, S.A., *Composites: Part B*, Vol. 37 (2006) pp.662–669.
10. Giannopoulos, G.I., Kakavas, P.A., Anifantis, N.K., *Computational Materials Science*, Vol. 41 (2008) pp. 561-569.
11. Ávila, A.F., Lacerda, G.S.R., *Material Research*, Vol. 11, No. 3 (2008) pp.325–33.
12. Rafiee, R., Heidarhaei, M., *Composite Structures*, Vol. 94 (2012) pp.2460–2464.
13. Lu, X., Hu, Zh., *Composites: Part B*, Vol. 43 (2012) pp.1902-1913.
14. Dresselhaus, M.S., Dresselhaus, G., Saito, R., *Carbon*, Vol. 33, No. 7 (1995) pp.883–91.
15. Gogotsi Y., Ed., 'Nanomaterials Handbook', CRC Press, Taylor & Francis Group, USA (2006).
16. Cornell, W.D., Cieplak, P., Bayly, C.I., Gould, I.R., Merz, K.M., Ferguson, D.M., et al., *J Am Chem Soc*, Vol. 117 (1995) pp.5179–97.
17. Wernik, J.M., Meguid, S.A., Acta Mech, Vol. 217 (2011) pp.1–16.
18. Shokrieh, M.M., Rafiee, R., *Materials and Design*, Vol. 31 (2010) pp. 790–795.
19. Ayatollahi, M.R., Shadlou, S., Shokrieh, M.M., *Composite Structures*, Vol. 93 (2011) pp. 2250–59.
20. Poncharal, P., Wang, Z.L., Ugarte, D., Heer, W.A., *Science*, Vol. 283 (1999) pp.1513–6.
21. Wong, E.W., Sheehan, P.E., Liebert, C.M., *Science*, Vol. 26 (1997) pp. 1971-75.
22. Wu, Y., Zhang, X., Leung, A.Y.T., Zhong, W., *Thin-walled Struct*, Vol. 44, No.6 (2006) pp. 667–676.